Available online at www.sciencedirect.com
ScienceDirect
Procedia Computer Science 00 (2010) 1–17
Procedia Computer Science

Probe Interval Designs that Improve Accuracy of CoMPACT Monitor

K. Watabe[a], Y. Honma[a], M. Aida[a]

[a]*The author are with the Graduate School of System Design, Tokyo Metropolitan University, Hino-shi 191-0065, Japan.*

Abstract

We have proposed the CoMPACT monitor; it achieves the scalable measurement of the one-way delay distribution for each flow. CoMPACT monitor transforms the one-way delay data obtained by active measurement by using the passively monitored traffic data of the target flow. A recent study reported that using an inter-probe time with Gamma distribution can improve the accuracy of simple active measurements. The improvement is in terms of the ensemble mean of the stationary stochastic process. In this paper, to improve accuracy of CoMPACT monitor, we apply Gamma-probing as the active measurement component of CoMPACT monitor. The significant issue in this application is in the difference between objects targeted for measurement; CoMPACT monitor estimates the time average of sample path rather than the ensemble mean. We investigate the characteristics of CoMPACT monitor and Gamma-probing, and verify the improved accuracy of CoMPACT monitor through simulations.

Keywords: QoS measurement, delay measurement, change-of-measure, Gamma distribution

1. Introduction

With the rapid growth of the Internet over the last few years, it has come to play an important role as a key social infrastructure. Various applications provide new services including telephony and live video on the Internet, and the traffic they stream exhibits complex characteristics. These various applications require various quality of service (QoS) guarantees and so differ from traditional e-mail and web browsing applications. Given that even more unusual applications will arise in the future, the diversification of QoS requirements can only strengthen.

In order to meet such the varied network control requirements, we need a measurement technology that can produce detailed QoS information. Measuring the QoS for each flow (e.g., users, applications, or organizations) is important since it is a key parameter in service level agreements

Email addresses: watabe-kouhei@sd.tmu.ac.jp (K. Watabe), yudai@sd.tmu.ac.jp (Y. Honma), maida@sd.tmu.ac.jp (M. Aida)

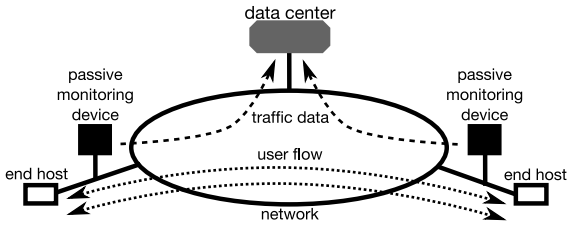

Figure 1: Two-point passive measurement

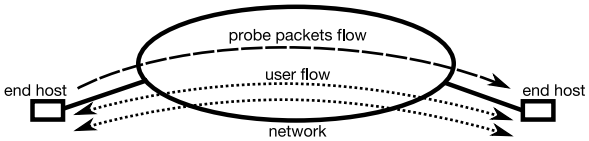

Figure 2: Active measurement

(SLAs) between the Internet service provider (ISP) and the user. One-way packet delay is one of the most important QoS metrics. This paper focuses on the measurement of one-way delay for each flow.

Many tools have been proposed to assess QoS including one-way delay ([1, 2]), and have also been evaluated in previous studies ([3, 4, 5]). Conventional techniques of measuring network performance and QoS can be classified as either passive or active measurements.

Passive measurement monitors the target user packet directly, by capturing the packets, including the target information (see Fig. 1). Passive measurement is used to measure the volume of traffic, one-way delay, round-trip time (RTT), loss, etc. It can get any desired information about the traffic since it observes the actual traffic. Passive measurement can be categorized into two-point monitoring with data-matching processes (to measure one-way delay etc.) and one-point monitoring (to measure the volume of traffic etc.).

Passive measurement has the advantage of accuracy. However, if we perform passive measurements in a large-scale network, the number of monitored packets is enormous, and network resources are wasted by gathering the monitored data at the data center. Moreover, in order to measure delay, it is necessary to determine the difference in arrival time of a particular packet at different points in the network. This requires searching for the packet which was recorded in the data monitored at one point from the data monitored at other point. This packet matching process lacks scalability, so passive measurement lacks scalability.

Active measurement monitors QoS by injecting probe packets into a network path and monitoring them (see Fig. 2 and [6, 7, 8, 9]). Active measurement can be used to measure one-way delay, RTT, loss, available bandwidth [10], etc. It cannot obtain the per-flow QoS, but this is easy for the end user to perform. Unfortunately, the QoS data obtained by active measurement does not represent the QoS of the user packets, only QoS of the probe packets.

The authors previously described how the advantages of active and passive measurements could be joined in their scalable measurement proposal called *c*hange-*o*f-*m*easure-based *p*assive/*act*ive *monitor*ing (CoMPACT monitor); it offers per-flow QoS measurement ([11, 12, 13]).

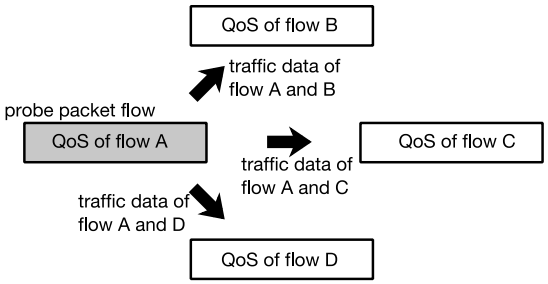

Figure 3: The transformation of QoS by CoMPACT monitor

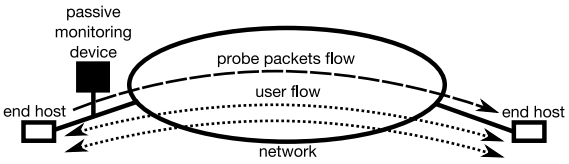

Figure 4: The composition of CoMPACT monitor

The idea of CoMPACT monitor is as follows. The direct measurement of QoS of the target flow by passive measurement is not really feasible due to the scalability problem. Instead, the QoS of the target flow is gained by transforming QoS data obtained by active measurement. The transformation reflects the passively monitored traffic data (volume of traffic) of the target flow (see Fig. 3). We show the composition of CoMPACT monitor in Fig. 4. The problem of scalability is well suppressed, because the volume of traffic can be measured by one-point passive measurement without requiring data-matching processes.

We original assumed that Poisson arrivals (intervals follow an exponential distribution) would be most appropriate for designing a policy of probe packet arrival since it permits the application of PASTA (Poisson Arrivals See Time Averages) property [14]. In addition, we applied the exponential distribution, as an inter-probe time distribution, in verifying CoMPACT monitor.

However, recent work [15] indicates that there maybe many distributions that are more accurate than an exponential distribution if a non-intrusive context (ignoring the existence of probe packets) can be assumed. Moreover, according to [16], we can find a distribution that is suboptimal in accuracy by setting the inter-probe time according to a parameterized Gamma distribution.

This paper confirms that applying Gamma-probing to CoMPACT monitor can improve its accuracy in measuring the one-way delay distribution of individual flows. The significant issue in this application lies in the difference between the objects targeted for measurement. In [16], the process observed by probe packets is assumed to be stationary and ergodic stochastic. This means that accuracy improvement is guaranteed only when the ensemble mean of a stationary stochastic process is estimated. However, CoMPCT monitor estimates the time average of the sampled path. Therefore, we should carefully investigate the characteristics of CoMPACT monitor with Gamma-probing.

The rest of the paper is organized as follows. We describe the concept and mathematical for-

mulation of CoMPACT monitor in section 2. Next, we briefly summarize the theory of Gamma-probing for active measurement in section 3. Section 4 discusses the difference in objects targeted between Gamma-probing and CoMPACT monitor. To confirm that the accuracy of CoMPACT monitor can be improved by Gamma-probing, we execute some simulations in section 5 and section 7. We conclude the paper in section 8.

2. Summary of CoMPACT monitor

2.1. The concept

CoMPACT monitor estimates an empirical QoS for the target flow by converting observed values of network performance at timing of probe packet arrivals into a measure of the target flow timing. Now, let $v(t)$ denote the network process under observation (e.g. the virtual one-way delay in the network path at time t), and X_k denote a random variable which is observed $v(t)$ with a certain timing (e.g. the timing of user k's packet arrivals). The probability of X_k exceeding c is

$$\begin{aligned}\Pr(X_k > c) &= \int 1_{\{x>c\}} \mathrm{d}F_k(x) \\ &= \mathrm{E}_{F_k}[1_{\{x>c\}}]\end{aligned}$$

where $F_k(x)$ and $1_{\{\cdot\}}$ denote, respectively, the distribution function of X_k and the indicator function, and E_{F_k} denotes the expectation with respect to F_k.

If we can directly monitor X_k, its distribution can be estimated by

$$\frac{1}{m}\sum_{n=1}^{m} 1_{\{X_k(n)>c\}}, \qquad \text{for sufficiently large } m.$$

where $X_k(n)$ $(n = 1, 2, \cdots, m)$ denotes the nth observed value of X_k. Now, let us consider the situation that X_k cannot be directly monitored (actually, we cannot directly monitor X_k by using passive measurement in large-scale networks). Let Y denote a random variable which is observed $v(t)$ with a different timing (e.g. timing of probe packet arrivals), independent of X_k. This forces us to consider the relationship between X_k and Y.

Observed values of X_k and Y are different if their timing is different, even if they observe a common process $v(t)$ (see Fig. 5). X_k and Y can be related by each distribution functions $F_k(x)$ and $G(y)$, and $\Pr(X_k > c)$ expressed by measure of X_k can be transformed into measure of Y as follows.

$$\begin{aligned}\Pr(X_k > c) &= \int 1_{\{x>c\}} \mathrm{d}F_k(x) \\ &= \int 1_{\{y>c\}} \frac{\mathrm{d}F_k(y)}{\mathrm{d}G(y)} \mathrm{d}G(y) \\ &= \mathrm{E}_G\left[1_{\{Y>c\}} \frac{\mathrm{d}F_k(Y)}{\mathrm{d}G(Y)}\right]\end{aligned}$$

where E_G denotes the expectation with respect to G.

Therefore, $\Pr(X_k > c)$ can be estimated by

$$\frac{1}{m}\sum_{n=1}^{m} 1_{\{Y(n)>c\}} \frac{\mathrm{d}F_k(Y(n))}{\mathrm{d}G(Y(n))}, \quad \text{for sufficiently large } m. \tag{1}$$

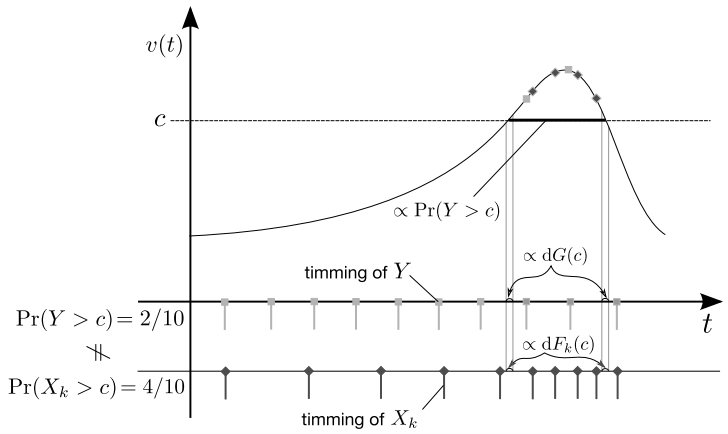

Figure 5: The relation between timing of arrivals and empirical QoS

where $Y(n)$ $(n = 1, 2, \cdots, m)$ denotes the nth observed value of Y. Note that this estimator does not need to know $X_k(n)$, if we can get $\mathrm{d}F_k(Y(n))/\mathrm{d}G(Y(n))$. This means the QoS of a specific flow (as decided by k) can be estimated by just one probe packet flow which arrives with timing of Y.

2.2. Mathematical formulation

This subsection briefly summarizes the mathematical formulation of the CoMPACT monitor with regard to one-way delay ([13]). We assume the traffic in the target flow can be treated as a fluid. In other words, we assume the target flow packets outnumber the active probe packets.

Let $a(t)$ and $v(t)$ denote, respectively, the traffic in the target flow at time t (≥ 0) and the virtual one-way delay on the path that we want to measure. $a(t)$ and $v(t)$ are nonnegative deterministic processes assumed to be right-continuous with left limits and bounded on $t \geq 0$. We can take $a(t)$ and $v(t)$ as sample paths of the corresponding stochastic processes.

Considering the measurement of the empirical one-way delay distribution $\pi(c)$, the value we want to measure is the ratio of traffic whose delay exceeds c to all traffic of the target flow, which is given by

$$\pi(c) = \lim_{t\to\infty} \frac{\int_0^t 1_{\{v(s)>c\}} a(s)\mathrm{d}s}{\int_0^t a(s)\mathrm{d}s}. \tag{2}$$

$\pi(c)$ can be estimated by estimator $Z_m(c)$ as follows (see [13] for details).

$$\begin{aligned} Z_m(c) &= \frac{1}{m}\sum_{n=1}^{m} 1_{\{v(T_n)>c\}} \frac{a(T_n)}{\sum_{l=1}^{m} a(T_l)/m} \\ &= \sum_{n=1}^{m} 1_{\{v(T_n)>c\}} \frac{a(T_n)}{\sum_{l=1}^{m} a(T_l)} \end{aligned} \tag{3}$$

for sufficiently large m, where T_n $(n = 1, 2, \cdots, m)$ denotes the nth sampling time, and each time of sampling corresponds to a time of probe packet arrival. Active and one-point passive

measurement are used to observe $v(T_n)$ and $a(T_n)$, respectively. Note that measuring the volume of traffic by one-point passive measurement is achieved much more easily than measuring the one-way delay by two-point passive measurement.

If we extract quantity $\sum_{n=1}^{m} 1_{\{v(T_n)>c\}}/m$ from equation (3), we can use it as a simple active estimator that counts the packets whose delay exceeds c. However, equation (3) is weighted by $a(T_n)/(\sum_{l=1}^{m} a(T_l)/m)$, which is decided by the traffic in the target flow when probe packets arrive. This means that the one-way delay distribution (measured by active measurement without bias) is corrected to the empirical one-way delay distribution by the bias of the target flow (observed by passive measurement). $a(T_n)/(\sum_{l=1}^{m} a(T_l)/m)$ in equation (3) corresponds to $\mathrm{d}F_k(Y(n))/\mathrm{d}G(Y(n))$ in equation (1).

Since the traffic is not really a fluid, we use the number of packets that are in the δ-neighborhood of T_n $[\max\{T_n - \delta/2, T_{n-1}\}, \min\{T_{n+1}, T_n + \delta/2\})$ instead of $a(T_n)$, where δ is a predefined small positive number ([13]).

3. Suboptimal probe intervals

3.1. NIMASTA

Since the PASTA property is good for non-biased measurement, Poisson arrivals (intervals follow an exponential distribution) have been widely used as the design policy of probe packet arrivals for active measurement. However, recent work [15] indicates that there may be many other distributions that can estimate the true value if a non-intrusive context (the effect of probe packets is ignored) can be assumed. This property was named NIMASTA (Non-Intrusive Mixing Arrivals See Time Averages) in [15].

NIMASTA contains three assumptions. First, the stochastic process that expresses the network state we are interested in (e.g. virtual delay) is stationary and ergodic. This process is called the ground truth process in [16]. Second, the point process of probe packets arrivals $\{T_n\}$ $(n = 1, 2, \cdots, m)$ is stationary and mixing. Mixing is the requirement to guarantee joint ergodicity between the probe and ground truth processes (see [15] for details). The last assumption is the non-intrusive context, i.e. we can ignore the impact of probe packets. Namely, the ratio of the probe stream to all streams is very small.

Under the above assumptions, [15] proved that the following equation holds.

$$\begin{aligned}\lim_{m\to\infty} \frac{1}{m} \sum_{n=1}^{m} f(Y(T_n)) &= \lim_{t\to\infty} \frac{1}{t} \int_0^t f(Y(t))\mathrm{d}t \\ &= \mathrm{E}[f(Y(0))] \qquad \text{a.s.,} \end{aligned} \tag{4}$$

where f and $Y(t)$ denote an arbitrary positive function and the ground truth process, respectively. Equation (4) means that we can estimate the ensemble mean of the ground truth process $\mathrm{E}[f(Y(0))]$ by using any probe packet policy if the point process of probe packet arrival $\{T_n\}$ is mixing. An example of the mixing point process has processes whose intervals follow the Gamma distribution and the uniform distribution. Note that periodic-probing with fixed intervals is not a mixing process, and does not satisfy equation (4).

3.2. Setting probe intervals to decrease variance

A recent study [16] reported that NIMASTA-based probing offers improved measurement accuracy. We can select a suboptimal (in terms of accuracy) probing process under a specific assumption by using the inter-probe time given by the parameterized Gamma distribution.

If we estimate the mean of $Y(0)$ by using active measurement, estimator $\hat{p}$ is

$$\hat{p} = \frac{1}{m}\sum_{n=1}^{m} Y(T_n). \tag{5}$$

Thus the variance of $\hat{p}$ is

$$\begin{aligned}
\mathrm{Var}[\hat{p}] &= \frac{1}{m^2}\mathrm{Var}\left[\sum_{n=1}^{m} Y(T_n)\right] \\
&= \frac{1}{m^2}\sum_{n=1}^{m}\mathrm{Var}[Y(T_n)] + \frac{2}{m^2}\sum_{n\neq l}\mathrm{Cov}\left(Y(T_n), Y(T_l)\right) \qquad (6)\\
&= \frac{1}{m}\mathrm{Var}[Y(0)] + \frac{2}{m^2}\sum_{n\neq l}\int R(\tau) f_{|n-l|}(\tau)\mathrm{d}\tau \qquad (7)
\end{aligned}$$

where f_k is probability density function (pdf) of T_k, $R(\tau) = \mathrm{Cov}\left(Y(t), Y(t-\tau)\right)$ is the autocovariance function (ACF) of the ground truth process $Y(t)$ (we can express $R(\tau, t)$ by τ alone, because $Y(t)$ is stationary) and the last equality follows from the stationary property of $Y(t)$ and the probe packet process.

If $R(\tau)$ is convex, the following can be proven by using Jensen's inequality. No other probing process with an average interval of μ has a variance that is lower than that of periodic-probing (see [16]). Estimator variance is connected with accuracy, lower is better, so periodic-probing is the best policy if we focus only on variance.

On the other hand, periodic-probing does not satisfy the assumptions of NIMASTA due to non-mixing, so periodic-probing is not necessarily the best. This is because a phase-lock phenomenon may occur and the estimator may converge on a false value when the cycle of the ground truth process corresponds to the cycle of the probing process. Namely, periodic-probing has a bias.

To tune the tradeoff between traditional policies obeying Poisson arrivals and periodic-probing (which has a bias but has the advantage in terms of variance), [16] proposes a suboptimal policy that gives an inter-probe time that obeys the parameterized Gamma distribution. The pdf that is used as the interval between probe packets is given by

$$g(x) = \frac{x^{\beta-1}}{\Gamma(\beta)}\left(\frac{\beta}{\mu}\right)^{\beta} \mathrm{e}^{-x\beta/\mu} \qquad (x > 0), \tag{8}$$

where $g(x)$ is the Gamma distribution whose shape and scale parameters are β and μ/β, respectively. μ (> 0) denotes the mean, and β (> 0) is the parameter. When $\beta = 1$, $g(x)$ reduces to the exponential distribution with mean μ. When $\beta \to \infty$, the policy reduces to periodic-probing because $g(x)$ converges on $\delta(x - \mu)$.

If ACF is convex, it has been proven that the variance of estimator $\hat{p}$ sampled by intervals that follow equation (8) monotonically decreases as β increases. This decrease is caused by the decrease of the covariance part which is the second term on the right-hand side of equation (7). We can achieve small variance (it approaches the variance of periodic-probing) by setting β to a large value since equation (8) converges on periodic-probing towards limit $\beta \to \infty$.

The problem of bias due to the phase-lock phenomenon can be avoided if we tune β to a limited value (the probing process that has intervals set by equation (8) is mixing). Resolving the tradeoff between a traditional policy that assumes Poisson arrivals and periodic-probing yields a suboptimal probing process if we give β an appropriate value.

4. The application to CoMPACT monitor

This section discusses the application of Gamma-probing to CoMPACT monitor. First, we must determine the ground truth process observed by CoMPACT monitor. Comparing equation (5) with equation (3), we can consider that stochastic process $Y(t)$ observed by CoMPACT monitor is

$$Y(t) = 1_{\{V(t)>c\}} \frac{A(t)}{\mathrm{E}[A(t)]} , \tag{9}$$

where $V(t)$ and $A(t)$ are stochastic processes corresponding to sample path $v(t)$ and $a(t)$, respectively. If it is confirmed that the ACF $R(\tau)$ of stochastic process $Y(t)$ is convex, we can guarantee an improvement in accuracy due to Gamma-probing by applying the theory in section 3.

The convexity of ACF has been verified for cases of simple virtual delay process and loss process using data of large-scale passive measurements and simulations ([16]). However, $Y(t)$ observed by CoMPACT monitor is weighted by traffic $A(t)$ of a specific flow, so the property of $Y(t)$ clearly differs from the delay/loss processes that are influenced by all flows on the network. Therefore, we must confirm the convexity of $R(\tau)$ in the CoMPACT monitor case. In section 5 and section 7, we will show that the assumption ($R(\tau)$ is convex) is appropriate to CoMPACT monitor.

As described in section 2, we consider $v(t)$ and $a(t)$ are sample paths of corresponding stochastic processes since CoMPACT monitor estimates the time average of sample path given by equation (2). However, as explained in section 3, the ground truth process $Y(t)$ is stationary stochastic process in [16], and the decrease of variance of $\hat{p}$ is guaranteed for the estimation of the ensemble mean of $Y(t)$. The variance of $\hat{p}$ depends on both stochastic variations of $Y(t)$ and T_n. On the other hand, CoMPACT monitor observe sample path $y(t)$ rather than stochastic process $Y(t)$, because CoMPACT monitor estimates one-way delay that is experienced by user flows.

Therefore, it is desired in CoMPACT monitor that variance of estimator $\hat{p}$ which depends only on sampling time T_n on certain sample path rather than $Y(t)$ decreases. In other words, variance we want to decrease is given by

$$\mathrm{Var}[\hat{p}] = \frac{1}{m^2} \sum_{n=1}^{m} \mathrm{Var}[y(T_n)] + \frac{1}{m^2} \sum_{n \neq l} \mathrm{Cov}(y(T_n), y(T_l)). \tag{10}$$

Note that equation (10) corresponds to equation (6). If the ACF of $Y(t)$ is convex, we can consider that the covariance part, which is the second term on the right-hand side of equation (10), tends to decrease as β increases. Thus the variance of inter-probe time given by equation (8) is μ^2/β; and it to decreases as β increases. Hence, we can also expect that the variance part, which is the first term on the right-hand side of equation (10), decreases as β increases since none of the observed values $y(T_n)$ vary. In section 5 and section 7, we will show that the variance of estimator which depends only on T_n decreases with increase of β by using Gamma-probing through the simulation.

5. The effectiveness of suboptimal probe intervals

5.1. Simulation model

We used NS-2 [17] based simulations to investigate the effectiveness of Gamma-probing in the framework of CoMPACT monitor. The network model we used in the simulation is shown in Fig. 6.

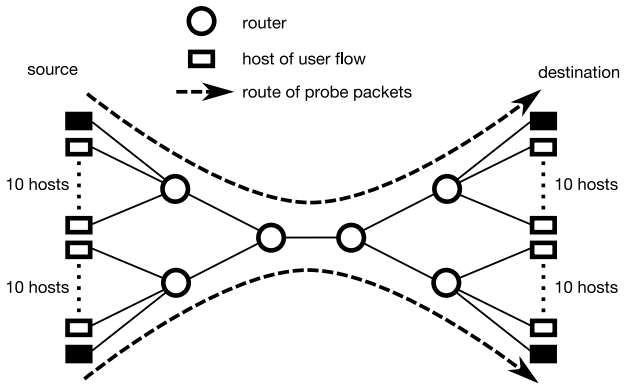

Figure 6: Network model

Table 1: Type of user flows

Flow type	Flow ID	Mean ON/OFF period	Distribution of ON/OFF length	Shape parameter	Rate at ON period
type 1	#1-5	10s/5s	Exponential	-	6 Mbps
type 2	#6-10	5s/10s	Exponential	-	6 Mbps
type 3	#11-15	5s/10s	Parete	1.5	9 Mbps
type 4	#16-20	1s/19s	Parete	1.5	9 Mbps

There are 20 pairs of source and destination end hosts. Each end host on the left in Fig. 6 is a source and transfers packets by UDP to the corresponding destination end host on the right. User flows are given as ON/OFF processes and categorized into the four types listed in TABLE 1; there are five flows in each type.

Probe packet flows are categorized into the five types listed in TABLE 2. Note that *Exponential* and *Deterministic* in TABLE 2 are special cases of Gamma distribution, and parameters of *Exponential* and *Deterministic* are parameters of the Gamma distribution corresponding to each probe type. 300 flows of each type are streamed over the two routes shown in Fig. 6, so the total number of probe packet flows in the network is 3000. To analyze the variance of the estimator, we streamed a large number of probe packet flows. Of course, we can estimate the empirical delay from just one probe packet in each flow.

User flow packets and probe packets are 1500 bytes and 64 bytes, respectively. Link capacities are identical at 64 Mbps. Delay occurs mainly in the link between the core routers, since it is a bottleneck, but no loss occurs, because there is sufficient buffering.

We observed the traffic by passive measurement at the queue of the edge router on the source side. Let δ denote 40 ms.

We ran the simulation for 500 s. The non-intrusive requirement (the effect of probe packets can be ignored) was satisfied, since the ratio of the probe stream to all streams is only 0.00197% or so.

5.2. The convexity of ACF

In this subsection, we will discuss whether the ACF of the ground truth process $Y(t)$ is convex. Note that the ground truth process is treated as stochastic process $Y(t)$, not sample path $y(t)$.

Table 2: Type of probe

Distribution of probe intervals	Parameter β	Mean probe intervals
Exponential	($\beta = 1$)	0.5 s
Gamma	$\beta = 5$	0.5 s
Gamma	$\beta = 25$	0.5 s
Gamma	$\beta = 125$	0.5 s
Deterministic (Periodic)	($\beta \to \infty$)	0.5 s

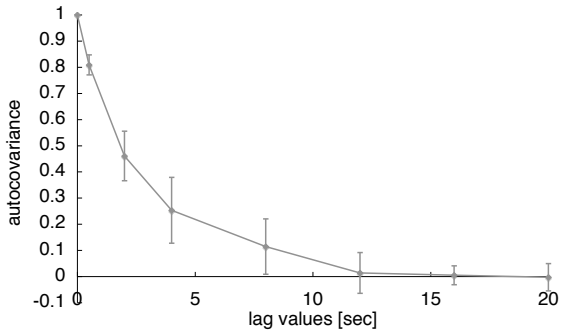

Figure 7: Autocovariance function (flow #1)

The ground truth process observed by CoMPACT monitor is given by equation (9). We compute $V(t)$, which is the virtual one-way delay, by using the queue occupancy (byte) of the core router on the source side. In our simulation model, the greatest part of the delay occurs at the core router on source side, because the link between the core routers is a bottleneck. Thus we can ignore any delay at other routers.

The (standardized) ACF for $c = 0.1$ for flow #1 with 95% confidence intervals on 10 experiments is depicted in Fig. 7. To plot Fig. 7, we used data where the queue occupancy and the traffic were recorded every 0.01 seconds. Representing each flow type, we also plotted flows #6, #11 and #16. This permitted the conclusion that none of these results contradicted the assumption that ACF is convex.

5.3. One-way delay distribution

In this subsection, we will show that CoMPACT monitor can estimate the empirical one-way delay by using Gamma-probing. The estimation of the complementary cumulative distribution function (CDF) of the one-way delay experienced by user flows (as given by equation (2)) will be shown below. Note that $v(t)$ and $a(t)$ are both sample paths in equation (2).

To estimate the complementary CDF of the one-way delay experienced by flow #1, we used probe packet flows with parameter $\beta = 1$, 25 and $\beta \to \infty$. Note that $\beta = 1$ corresponds to traditional PASTA-base probing. Each result, with 95% confidence intervals, is shown in Fig. 8. Note that the horizontal axis, which is the one-way delay, corresponds to c in equation (2). To compare the empirical delay with the estimate from CoMPACT monitor, we include the estimate from active measurement in the plot.

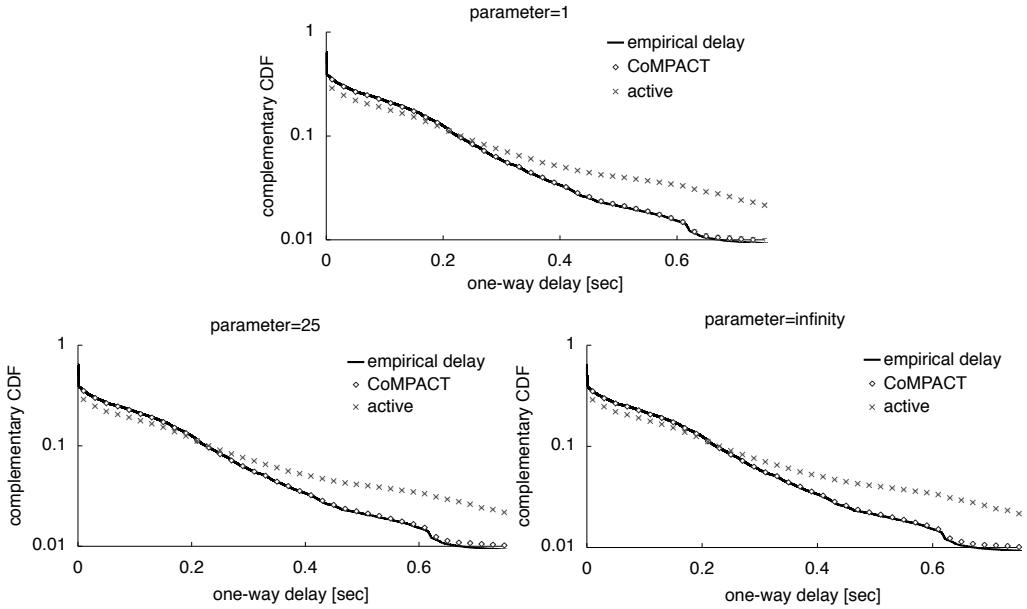

Figure 8: The estimation of comprementary CDF (flow #1)

In Fig. 8, we can see that the CoMPACT monitor gives good estimates of the true value. We cannot judge the superiority or inferiority of any type of probe packet flows. Representing each flow type, we have plotted for flows #6, #11 and #16 and similar results are gained.

5.4. Accuracy Improvement of CoMPACT monitor

In this subsection, we will verify the relationship between the parameter of Gamma distribution, used as the inter-probe time, and the variance of estimator. Note that we consider the variance of $\hat{p}$, which depends only on probe packet timing (namely, sampling time T_n).

We plot the standard deviation of each point of the complementary CDF (shown in subsection 5.3) in Fig. 9. Note that the horizontal axis corresponds to the one-way delay, which is c in equation (2). Error bars indicate the 95% confidence intervals when the standard deviation calculated from 30 probe packet flows is considered to be a single data point.

The standard deviation clearly decreases as β increases from $\beta = 1$ to $\beta = 125$. Note that $\beta = 1$ corresponds to traditional PASTA-base probing. In periodic-probing, i.e. $\beta \to \infty$, the standard deviation is often larger than that with $\beta = 125$ or $\beta = 25$. Our belief is that this reversal is a sign of the phase-lock phenomenon, which occurs when the cycle of the ground truth process corresponds to the cycle of the probing process. In section 6, we verify phase-lock phenomenon in detail. We got similar results for other flows though Fig. 9 shows only the results of flow #1 and #11.

Consequently, it was confirmed that we can obtain adequate accuracy on variance, which depends only on sampling time T_n with a suboptimal probing process, if we tune the parameter of Gamma distribution, which is used as the inter-probe time.

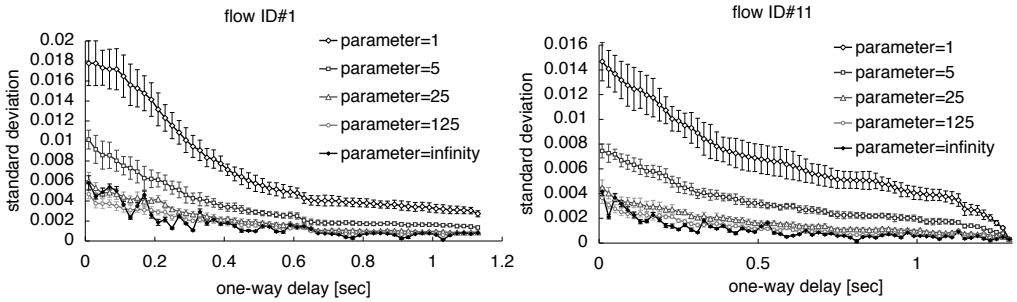

Figure 9: Standard deviation of estimator

5.5. The upper bounds of variance

Supplementing the simulation results in previous subsection, we prove that periodic-probing is assuredly superior to the traditional PASTA-based probing.

Let us idealize the traffic process $a(t)$ as an ON/OFF process. We assume $a(t)$ is the binary process which takes value α if the target flow streams, and 0 otherwise. Thus $\hat{p}$ is expressed by

$$\begin{aligned}\hat{p} = \sum_{n=1}^{m} 1_{\{v(T_n)>c\}} \frac{a(T_n)}{\sum_{l=1}^{m} a(T_l)} &= \sum_{n=1}^{m} 1_{\{v(T_n)>c\}} \frac{\alpha \cdot 1_{\{a(T_n)>0\}}}{\sum_{l=1}^{m} \alpha \cdot 1_{\{a(T_l)>0\}}} \\ &= \frac{\sum_{n=1}^{m} 1_{\{v(T_n)>c \wedge a(T_n)>0\}}}{\sum_{l=1}^{m} 1_{\{a(T_l)>0\}}}. \end{aligned} \tag{11}$$

Since UDP does not control the volume of traffic, this assumption is appropriate for UDP flows.

Now, we consider the range of equation (11). $1_{\{v(t)>c \wedge a(t)>0\}}$ and $1_{\{a(t)>0\}}$ are the binary processes, and we can divide them into the periods in which the processes take 0 and 1. If they are observed by periodic-probing, the difference between the maximum and minimum observation frequency is 1 at most in one period (see Fig. 10).

The maximum range Δ of equation (11) is given by

$$\Delta = \frac{k_2}{mq - k_1}, \tag{12}$$

where k_1 and k_2 denote the number of periods of $1_{\{a(t)>0\}} = 1$ and $1_{\{v(t)>c \wedge a(t)>0\}} = 1$, respectively, and q denotes the time average of $1_{\{a(t)>0\}}$.

The distribution that has maximum variance with range Δ has the following pdf $h(x)$.

$$h(x) = \frac{1}{2}\delta(x - a) + \frac{1}{2}\delta(x - a - \Delta),$$

where $\delta(\cdot)$ denotes Dirac δ function and a is an arbitrary constant. Therefore, the upper bounds of estimator variance are as follows.

$$\begin{aligned}\mathrm{Var}[\hat{p}] &\leq \left(\frac{\Delta}{2}\right)^2 \\ &= \frac{{k_2}^2}{4(mq - k_1)^2}. \end{aligned} \tag{13}$$

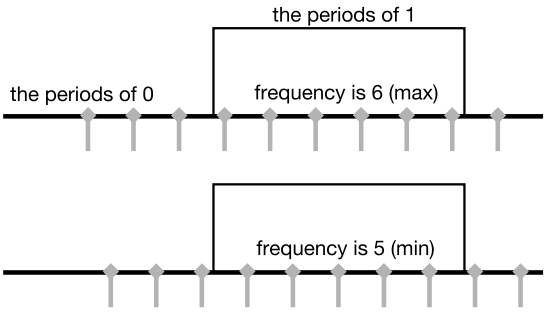

Figure 10: The observation frequency of periodic-probing

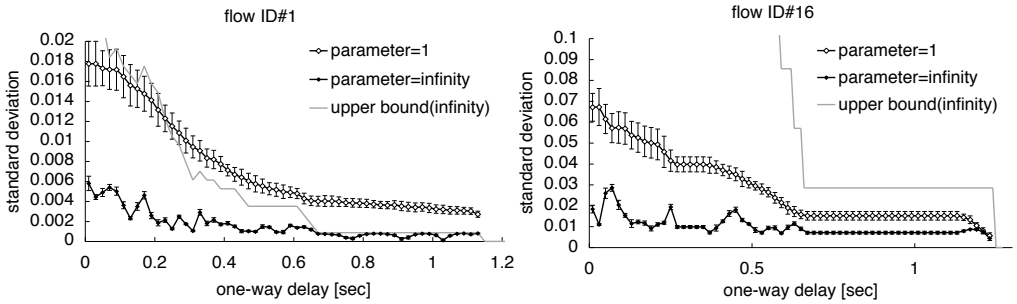

Figure 11: The upper bounds of periodic-probing

Calculating k_1, k_2 and q in the above simulation, we plot the upper bounds of periodic-probing in Fig. 11. Note that standard deviations of PASTA-based probing and periodic-probing (the same data as plotted in Fig. 9) are displayed.

The results of flow #1 confirm that the upper bounds of periodic-probing are smaller than the standard deviation of PASTA-based probing in the domain of interest (the domain with large delay). Therefore, it is guaranteed that periodic-probing is surely superior to PASTA-based probing. The results of flows #6, #11 (not displayed in Fig. 9) are similar to the results of flow #1.

The results of flow #16 show that the upper bounds of periodic-probing are larger than the standard deviation of PASTA-based probing because the combination of flow type 4 (e.g. flow #16) and equation (13) is bad. The type 4 flows have short ON periods and long OFF periods as shown in TABLE 1. Thus the maximum range given by equation (12) becomes large because the denominator becomes small. Therefore, the appropriate upper bounds cannot be given by equation (13).

6. Phase-lock phenomenon

In this section, we will discuss the phase-lock phenomenon in sample path observation. We will show that the accuracy reversal between periodic-probing ($\beta \to \infty$) and Gamma-probing ($\beta = 125$) in Fig. 9 occurs because periodic-probing locks the phase of the ground truth process.

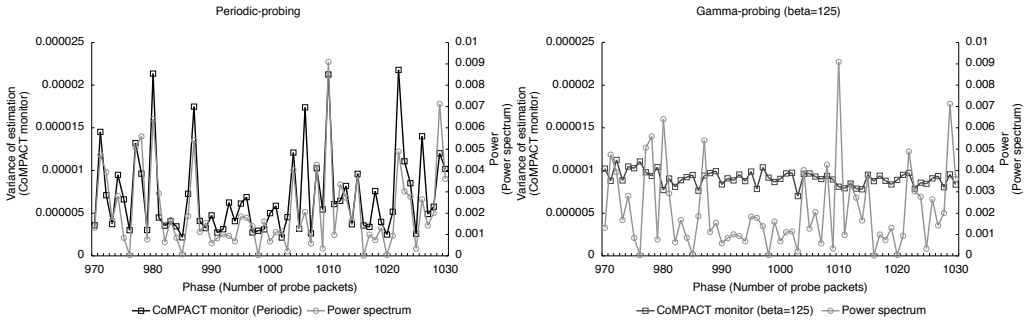

Figure 12: Power spectrum and variance of estimator

Convex ACF means that the ground truth process does not have any specific periodicity. If the ACF is strictly convex, the variance of estimator with periodic-probing is minimum as described in section 3.

However, there is the possibility that sample path $y(t)$ has, over a finite interval, *accidental periodicity*, even if the ACF of the ground truth process $Y(t)$ is convex. This is because the sample path over a finite interval fails to well represent the characteristics of the corresponding stochastic process. Namely, it is possible that the sample path has, over a short time, some specific periodicity by chance, even if there is no specific periodicity over the long term. This accidental periodicity destroys the convexity of ACF with regard to the time average and thus causes the phase-lock phenomenon. If the interval in which we want to measure QoS is sufficiently long, the phase-lock phenomenon will not happen because the ACF of $y(t)$ over the long term converges on the ACF of $Y(t)$ in the meaning of ensemble mean (we must assume that $Y(t)$ is ergodic). Therefore, the phase-lock phenomenon is possible with finite observation intervals.

To verify the relation between accidental periodicity and accuracy, we altered the simulation described in section 5. All conditions were unchanged except for the characteristics of probe packets which were altered as follows. The parameter of inter-probe time was set at $\beta \to \infty$ (periodic-probing) and $\beta = 125$. We examined probe packets with 61 different inter-probe times (namely 61 kinds of periodicity). Mean number of probe packets in the 500 s simulation (corresponding to m) ran from 970 to 1030 (e.g. if mean number of probe packets is 1000, the mean inter-probe time is 500 s / 1000 packet = 0.5 s).

We estimated one-way delay by probe packet flows which have 61 kinds of periodicity, and compared the variance of estimator with the power spectrum of the sample path over the simulation time $|\mathcal{F}[y(t)]|^2$ $(0 \le t < 500)$ ($\mathcal{F}[\cdot]$ denotes Fourier transform and power spectrum refers to the energy of each frequency component). The result for flow #1 is shown in Fig. 12. Note that we used 0.1s as the threshold of one-way delay c.

We can see that periodic-probing yields high estimator variance at the points with strong periodicity, which is indicated by power spectrum of finite time sample path. On the other hand, variance of estimator by Gamma-probing does not depend on the power spectrum. Therefore, the phase-lock phenomenon, which happens because probing locks due to accidental periodicity within a finite time sample path, was confirmed even if the ACF of the ground truth process is convex (namely the ground truth process does not have any specific periodicity).

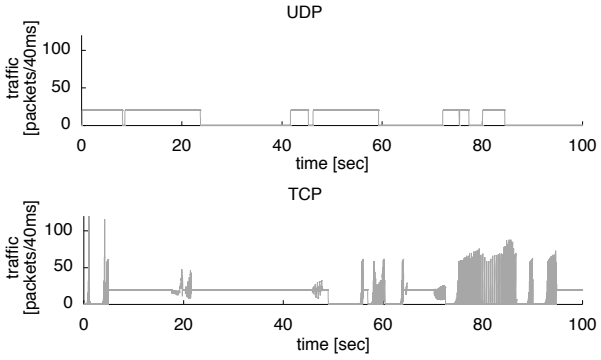

Figure 13: Traffic process

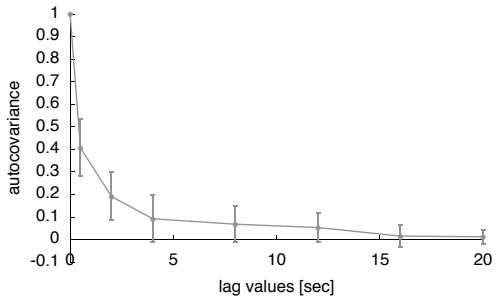

Figure 14: Autocovariance function in the case of TCP

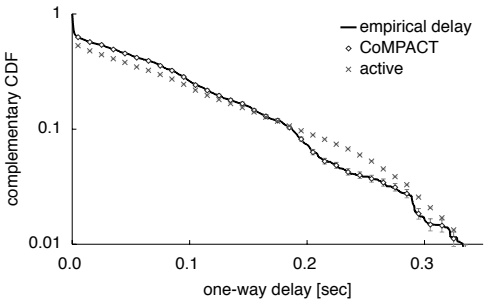

Figure 15: The estimation in case of TCP

7. Additional simulation

We used UDP flows in the simulation of section 5, but we also simulated the network carrying TCP flows. We used the same conditions as used in section 5, expect for replacing UDP flows with TCP flows. 300 packets was specified as the maximum window size.

In the case of TCP, user traffic is strongly affected by TCP traffic control. Therefore, the observed traffic of a TCP flow can differ greatly depending on the timing of the sampling, unlike UDP. A key characteristic of this simulation is that user traffic is very unstable (see Fig. 13). Comparing these results with those from the UDP simulation allows us to confirm whether Gamma-probing can be applied to flows with unstable traffic, or not.

In fact, we were able to confirm that the ACF of the ground truth process was convex and that the estimator converged on the true value, as in the UDP simulation. The ACF for $c = 0.1$ for flow #11 with 95% confidence intervals taken over 15 experiments is depicted in Fig. 14. The result of the estimation for flow #16 by using probe packets with parameter $\beta = 25$ is shown in Fig. 15. The traffic control of TCP has no negative effect on the convexity of ACF.

However, the standard deviation of the estimator was slightly different from that in the UDP simulation. Fig. 16 shows a plot of the standard deviation of each point versus the corresponding CDF point. The error bars indicate 95% confidence intervals with the standard deviation calculated from 30 probe packet flows taken to be a single datum, as in the UDP simulation.

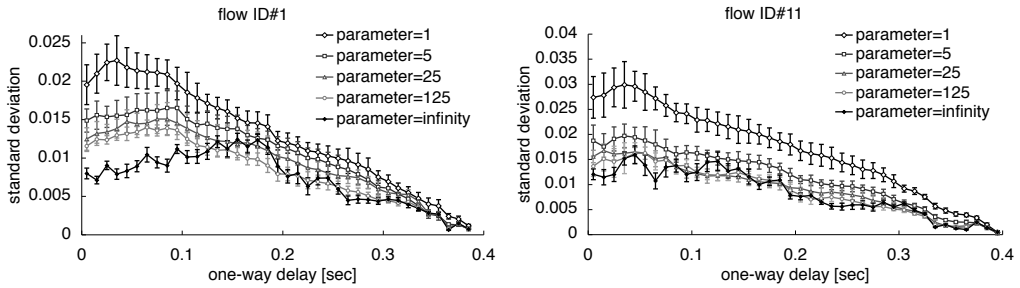

Figure 16: Standard deviation of estimator in the TCP case

We can confirm that there is no significant difference. There is a tendency to decrease from $\beta = 1$ to $\beta = 125$, but confidence intervals overlap each other. This overlap is caused by traffic instability. The variance of estimator is not steady when the target flow has strongly variable traffic. To stabilize the variance of estimator, we should set a longer observation period compared to the UDP case. However, we can well judge the tendency as regards the accuracy improvement from Fig. 16.

Now let us focus on $\beta \to \infty$ (corresponding to periodic-probing) in Fig. 16. The phase-lock phenomenon can be observed quite clearly by comparing these results with those of the UDP simulation. A clear reversal of the standard deviation is observed only with periodic-probing. This is the same as in the UDP simulation, though the reversal does not always happen. This result proves that periodic-probing is not optimal, even when the variance depends only on probe packet timing.

8. Conclusion

In a non-intrusive context where the effect of probe packets can be ignored, it was confirmed that the accuracy of estimating the complementary CDF of one-way delay can be improved by using Gamma-probing as part of determining CoMPACT monitor estimates. This means that the Gamma-probing proposed in [16] can be useful added to CoMPACT monitor for estimating the time average of sample paths.

The requirement that assures the achievement of accuracy improvement was clarified. [16] assumed that the ACF of a stochastic process taken to express the network state is convex. Using CoMACT monitor, we elucidated the stochastic process that expresses the network state and were able through simulations to confirm that its ACF is convex. The stochastic process observed by CoMPACT monitor depends on the traffic process of the observed flow. Compared to simple delay/loss processes, which are influenced by all traffic in the network, the traffic process of a specific flow sometimes exhibits periodicity. When we apply Gamma-probing to a real network, the convexity of ACF requires special attention because periodicity can destroy the convexity of ACF. The convexity contributes to the accuracy improvement possible when we estimate not only the ensemble mean of stochastic processes but also the time average of sample paths.

We have not addressed the issue of how to tune parameter β of Gamma-probing and it remains as a key future task.

References

[1] CAIDA: The Cooperative Association for Internet Data Analysis `http://www.caida.org/`.

[2] V. Paxson, J. Mahdavi, A. Adams, M. Mathis, An architecture for large scale internet measurement, IEEE Communications Magazine 36 (8) (1998) 48–54.

[3] J. Bolot, Characterizing End-to-End Packet Delay and Loss in the Internet, Journal of High Speed Networks 2 (1993) 305–323.

[4] V. Paxson, End-to-end Internet packet dynamics, IEEE ACM Trans Networking 7 (3) (1999) 277–292.

[5] S. Savage, A. Collins, E. Hoffman, J. Snell, T. Anderson, The end-to-end effects of Internet path selection, ACM SIGCOMM Computer Communication Review 29 (4) (1999) 289–299.

[6] G. Almes, S. Kalidindi, M. Zekauskas, A one-way delay metric for IPPM, RFC2679 (1999).

[7] G. Almes, S. Kalidindi, M. Zekauskas, A one-way packet loss metric for IPPM, RFC2680 (1999).

[8] A. Pásztor, D. Veitch, High precision active probing for Internet measurement, in: Proceedings of INET 2001, 2001.

[9] V. Paxson, G. Almes, J. Mahdavi, M. Mathis, Framework for IP Performance Metrics, RFC2330 (1998).

[10] M. Jain, C. Dovrolis, End-to-End Available Bandwidth: Measurement Methodology, Dynamics, and Relation with TCP Throughput, in: Proceedings of ACM SIGCOMM 2002, 2002, pp. 295–308.

[11] M. Aida, N. Miyoshi, K. Ishibashi, A scalable and lightweight QoS monitoring technique combining passive and active approaches, in: Proceedings of IEEE INFOCOM 2003, 2003, pp. 125–133.

[12] K. Ishibashi, M. Aida, S. Kuribayashi, Proposal and evaluation of method to estimate packet loss-rate using correlation of packet delay and loss, IEICE Transactions on Information and Systems E86-D (11) (2003) 2371–2379.

[13] M. Aida, N. Miyoshi, K. Ishibashi, A Change-of-Measure Approach to Per-Flow Delay Measurement Combining Passive and Active Methods: Mathematical Formulation for CoMPACT Monitor, IEEE Transactions on Information Theory 54 (11) (2008) 4966–4979.

[14] R. Wolff, Poisson arrivals see time averages, Operations Research 30 (2) (1982) 223–231.

[15] F. Baccelli, S. Machiraju, D. Veitch, J. Bolot, The role of PASTA in network measurement, ACM SIGCOMM Computer Communication Review 36 (4) (2006) 231–242.

[16] F. Baccelli, S. Machiraju, D. Veitch, J. Bolot, On optimal probing for delay and loss measurement, in: Proceedings of the 7th ACM SIGCOMM conference on Internet measurement, 2007, pp. 291–302.

[17] The Network Simulator – ns-2 `http://moat.nlanr.net/`.